Coherence and population dynamics of chlorophyll excitations in FCP complex: Two-dimensional spectroscopy study

Vytautas Butkus, Andrius Gelzinis, Ramūnas Augulis, Andrew Gall, Claudia Büchel, Bruno Robert, Donatas Zigmantas, Leonas Valkunas, and Darius Abramavicius

---

Articles you may be interested in

Communication: Coherences observed in vivo in photosynthetic bacteria using two-dimensional electronic spectroscopy
J. Chem. Phys. **143**, 101101 (2015); 10.1063/1.4930539

Influence of weak vibrational-electronic couplings on 2D electronic spectra and inter-site coherence in weakly coupled photosynthetic complexes
J. Chem. Phys. **143**, 065101 (2015); 10.1063/1.4928068

Probing energy transfer events in the light harvesting complex 2 (LH2) of Rhodobacter sphaeroides with two-dimensional spectroscopy
J. Chem. Phys. **139**, 155101 (2013); 10.1063/1.4824637

Two-dimensional electronic spectroscopy of bacteriochlorophyll a in solution: Elucidating the coherence dynamics of the Fenna-Matthews-Olson complex using its chromophore as a control
J. Chem. Phys. **137**, 125101 (2012); 10.1063/1.4752107

Signatures of correlated excitonic dynamics in two-dimensional spectroscopy of the Fenna-Matthew-Olson photosynthetic complex
J. Chem. Phys. **136**, 104505 (2012); 10.1063/1.3690498

Coherence and population dynamics of chlorophyll excitations in FCP complex: Two-dimensional spectroscopy study

Vytautas Butkus,[1,2] Andrius Gelzinis,[1,2] Ramūnas Augulis,[2] Andrew Gall,[3] Claudia Büchel,[4] Bruno Robert,[3] Donatas Zigmantas,[5] Leonas Valkunas,[1,2] and Darius Abramavicius[1,a)]

[1]*Department of Theoretical Physics, Faculty of Physics, Vilnius University, Sauletekio Ave. 9-III, 10222 Vilnius, Lithuania*
[2]*Center for Physical Sciences and Technology, Savanoriu Ave. 231, 02300 Vilnius, Lithuania*
[3]*Institut de Biologie et Technologies de Saclay, Bât 532, Commissariat à l'Energie Atomique Saclay, 91191 Gif sur Yvette, France*
[4]*Institut für Molekulare Biowissenschaften, Universität Frankfurt, Max-von-Laue-Straße 9, Frankfurt, Germany*
[5]*Department of Chemical Physics, Lund University, P.O. Box 124, 22100 Lund, Sweden*

Energy transfer processes and coherent phenomena in the fucoxanthin–chlorophyll protein complex, which is responsible for the light harvesting function in marine algae diatoms, were investigated at 77 K by using two-dimensional electronic spectroscopy. Experiments performed on femtosecond and picosecond timescales led to separation of spectral dynamics, witnessing evolutions of coherence and population states of the system in the spectral region of Q_y transitions of chlorophylls *a* and *c*. Analysis of the coherence dynamics allowed us to identify chlorophyll (Chl) *a* and fucoxanthin intramolecular vibrations dominating over the first few picoseconds. Closer inspection of the spectral region of the Q_y transition of Chl *c* revealed previously not identified, mutually non-interacting chlorophyll *c* states participating in femtosecond or picosecond energy transfer to the Chl *a* molecules. Consideration of separated coherent and incoherent dynamics allowed us to hypothesize the vibrations-assisted coherent energy transfer between Chl *c* and Chl *a* and the overall spatial arrangement of chlorophyll molecules. © *2015 AIP Publishing LLC.* [http://dx.doi.org/10.1063/1.4914098]

I. INTRODUCTION

Diatoms are unicellular chromophyte algae inhabiting marine environment. They are the major players in photosynthesis, accounting for nearly a quarter of the global primary production.[1–3] Light-harvesting in diatoms is performed by intrinsic membrane proteins, such as the fucoxanthin–chlorophyll protein (FCP) complex. FCP shares some structural and sequence homology with the light-harvesting complex II (LHCII) from the higher plants[4] but contains more carotenoids per chlorophyll (Chl). Carotenoids fucoxanthins (Fxs) strongly absorb blue–green photons with the longest propagation distances in water. Such adaptation allows diatoms to efficiently harvest sunlight in underwater conditions.

Information on the molecular structure of FCP is very limited; there are no crystallographic data of the complex. Several preliminary models of pigment organization in FCP, based on the assumption that the structure of FCP is similar to LHCII, have been proposed.[5–8] These models, however, are currently limited for several reasons. First, only some pigment binding sites are conserved between FCP and LHCII. Second, pigment composition and, thus, detailed functional roles in LHCII and FCP are markedly different, as the latter contains nearly as many fucoxanthin molecules as chlorophylls—most probably 8 Fx, 8 Chl *a*, and 2 Chl *c* molecules[7,9]—while LHCII is composed of 8 Chl *a*, 6 Chl *b*, and 4 xanthophyll molecules.[10]

Chl *c* molecules enhance the absorption of blue photons in FCP, as well.[11] Ultrafast molecular excitation transfer from Chl c to Chl *a* molecules was shown to occur at room temperature.[12] Nonetheless, the whole picture of the energy funnels in the FCP complex and the physical phenomena ensuring ultrafast energy transfer still needs to be detailed. Unfortunately, lack of structural information about FCP prevents detailed numerical studies. All the information about the inner workings of this complex comes solely from the experimental results and their analysis, which is often done in the light of the proposed models.[5–8] Therefore, it is important to obtain as much experimental data as possible to constrain and refine the current models.

The two-dimensional (2D) electronic spectroscopy (ES) is a remarkable tool for the analysis of coherent and incoherent phenomena appearing in molecular excitation dynamics. The first and the most recognized results of 2D ES demonstrating complex behavior of the excitation evolution were delivered for the photosynthetic Fenna–Matthews–Olson (FMO) complex from purple bacteria.[13] Since then, 2D ES has been successfully applied for studies of a number of different systems; 2D ES essentially helped to establish or update existing kinetic schemes of light-harvesting antennae and reaction centers of plants[14–17] and bacteria.[18–20] The 2D ES was also performed on the whole photosystem I complex demonstrating signatures of fast energy transfer.[21] In addition, it was utilized in studies of other molecular aggregates, for instance, polymers,[22] cylindrical (bi-tubular) J-aggregates,[23] and quantum dots.[24]

a)Electronic mail: darius.abramavicius@ff.vu.lt

142, 212414-1

Most of these findings were obtained from experiments and theoretical simulations performed using (or assuming) the knowledge of structural organization of the pigment molecules (often with resolution of a few angströms). Thus, these studies were valuable not only for widening a general understanding of the physical mechanisms within molecular systems but also were convenient for testing and interpreting the outcomes of the new method of 2D ES. As the method itself has already been well approved and appreciated, it becomes useful to apply the developed tools of analysis of the 2D spectra for more obscure molecular systems, for instance the FCP complex, and try to obtain more information about their structure/composition.

Recently, a few multidimensional spectroscopy studies of FCP reported valuable insight into various unknown characteristics of the complex. A novel method of two-color two-dimensional spectroscopy allowed to map the carotenoid–chlorophyll energy transfer pathways and resolved spectral heterogeneity of carotenoids in FCP.[25] It was found, that fucoxanthins in FCP are spectrally distinguishable and yet transfer energy to chlorophylls very efficiently. In our recent study,[12] dynamics of the two-dimensional spectra of Chl *a* and Chl *c* Q_y absorption bands at room temperature revealed ultrafast energy transfer between Chl *c* and Chl *a* with signatures of excitonic coupling. However, limited temporal and spectral resolutions in these particular experiments did not provide the possibilities to fully resolve coherent dynamics or a more fine structure of the FCP spectrum.

Here, we analyze results of the 2D ES of FCP obtained with a higher spectral and temporal resolution than in our previous work.[12] To better discriminate the weak spectral features of FCP, experiments were carried out at 77 K instead of room temperature. The 2D spectra were recorded with both femtosecond and picosecond time steps, thus, providing us the possibility to separate coherent and incoherent processes. In this work, we show that there are at least two Chl *c* molecules in FCP, which are clearly spectrally resolvable and participate in energy transfer on remarkably different timescales. We discuss that this might be related to a certain spatial arrangement of Chl *a* and *c* molecules in the complex. Finally, the analysis of rich coherent dynamics during the first picosecond reveals signatures of Chl *a* and fucoxanthin intramolecular vibrations, the former of which might play a role in enhancing the ultrafast Chl *c*-to-*a* energy transfer.

II. MATERIALS AND METHODS

Fucoxanthin–chlorophyll protein complexes were extracted and purified from diatom *Cyclotella meneghiniana*. The procedure of purification and extraction is given in detail in Ref. [26]. The sample for the measurements was diluted with the glycero–buffer–detergent solution (10 mM Mes pH 6.5 buffer, 2 mM KCl, 0.03% (w/v) n-Dodecyl β-D-maltoside, and 60% (v/v) glycerol) to achieve optical density of about 0.3 at Chl *a* Q_y band in 0.5 mm cell. The sample was placed in a 0.5 mm quartz cell and gradually cooled to 77 K in a liquid N_2 bath cryostat (Oxford Instruments).

The setup for coherent two-dimensional electronic spectroscopy was based on the inherently phase-stabilized design by Brixner *et al.*[27] In more detail, 10 fs, 100 nm full width at half maximum (FWHM) light pulses (3 nJ energy per pulse at the sample) centered at 615 nm were generated by the homebuilt non-collinear optical parametric amplifier pumped by the Yb:KGW amplified laser system ("Pharos," Light Conversion Ltd.) with repetition rate reduced to 7 kHz by means of the pulse picker. Diffractive-optics-based non-collinear four-wave mixing setup with phase-matched box geometry was used. The third-order signal was obtained by spectral interferometry with the help of a heterodyning local-oscillator pulse. Sensitivity and noise resistance was significantly enhanced by means of double modulation lock-in detection.[28] Coherence time delay was scanned within −140–300 fs time range with 2 fs time step controlled by movable fused-silica wedges in beams $\vec{k}_1$ and $\vec{k}_2$. 2D spectra were obtained by processing the accumulated sequence by the Fourier transform method.[29] The absolute phase of the 2D spectrum was retrieved by matching its projection with the transient absorption spectrum[30] recorded with the same setup with only two beams (for pump and probe) in use. Real (absorptive) parts of the rephasing + nonrephasing spectra were used in the further analysis.

III. RESULTS

The absorption spectrum of FCP measured at 77 K is shown in Fig. 1 by the black solid line. The spectrum contains a well expressed band at 14 895 cm^{-1} and a few weaker features around 15 700 cm^{-1} and 17 000 cm^{-1}. The dominating band at 14 895 cm^{-1} is known to represent the Q_y transition of the core pigment Chl *a*. The feature at 15 680 cm^{-1} was assigned to the Q_y transition of Chl *c*, while the origin of bands at around 16 200 cm^{-1} and 17 000 cm^{-1} was discussed to be reflecting the Q_x transitions of Chl *a* and Chl *c*, respectively.[12]
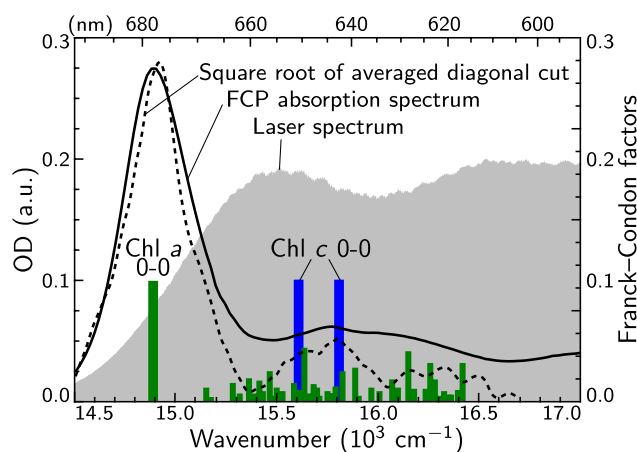

FIG. 1. The absorption spectrum of FCP at 77 K (solid black line), square root of averaged (delay times from t_2 = 30 fs to 800 fs) diagonal cut of the 2D spectrum (dashed black line), excitation laser spectrum of 2D ES experiment (filled gray area). Thicker vertical green and blue sticks indicate the energies of the 0–0 Q_y transitions of Chl *a* and Chl *c*, respectively. Vibrational states of Chl *a*, proposed by the hole burning measurements,[31] are shown by thinner green vertical sticks. Their heights indicate the Franck–Condon factors of the corresponding vibrations (values on the right axis).

The spectrum of the laser pulse used in the 2D ES experiment is shown by a gray shaded area in Fig. 1. The spectrum was centered at around $16\,240\,\mathrm{cm^{-1}}$ with the FWHM of $\sim 2600\,\mathrm{cm^{-1}}$. The laser spectrum was intentionally shifted to the blue to enhance the signals from the weak absorption bands of FCP: while it only partly covered the main absorption band at $14\,895\,\mathrm{cm^{-1}}$, the other weak features were fully covered by the laser spectrum.

Two different 2D ES experiments were carried out. In the first one, the 2D spectra at delay times t_2 up to 800 fs were taken at every 10 fs. Such a high temporal resolution is very useful for the analysis of the ultrafast excitation transfer dynamics as well as for studies of the quantum coherences and allowed us to resolve coherent beatings up to $1668\,\mathrm{cm^{-1}}$ in the frequency domain. The second set of data consisted of the 2D spectra measured at delay times t_2 up to 1 ns with different time steps: from 50 fs for the initial evolution to 100 ps for delay times longer than 100 ps. These measurements were used for the analysis of the incoherent long-time population dynamics in FCP.

A few 2D spectra at different delay times ($t_2 = 30$ fs, 330 fs, 5 ps, and 30 ps) are depicted in Fig. 2(a). In the

spectra, the main band corresponding to the Chl *a* transition at $\omega_3 = \omega_1 = 14\,926\,\mathrm{cm^{-1}}$ dominates. The fact that the band is not observed exactly at $14\,895\,\mathrm{cm^{-1}}$ as in the absorption spectrum, but rather blue-shifted by $31\,\mathrm{cm^{-1}}$ is caused by the excitation laser spectrum being slightly off-resonant with respect to the main FCP absorption band (see Fig. 1). The negative excited state absorption is well resolved above the diagonal in the 2D spectrum in the vicinity of the main positive absorption peak. The excited state absorption features in the 2DES could arise both due to excitonically coupled pigments (chlorophylls) and the corresponding double-excitation transitions,[32–34] as well as from the double-excitations of chlorophylls themselves.[35]

In the 2D spectra shown in Fig. 2(a), thinner contour lines, drawn at every 2% of the maximum highlight the fine structure of the diagonal and off-diagonal peaks (cross-peaks) away from the main Chl *a* absorption band. The most pronounced features correspond to the cross-peaks lying around the same emission frequency ω_3 as the Chl *a* absorption band. These peaks might either signify the excitonic coupling between Chls *a* and *c*,[12] or they might be caused by the Chl *a* vibrational modes.
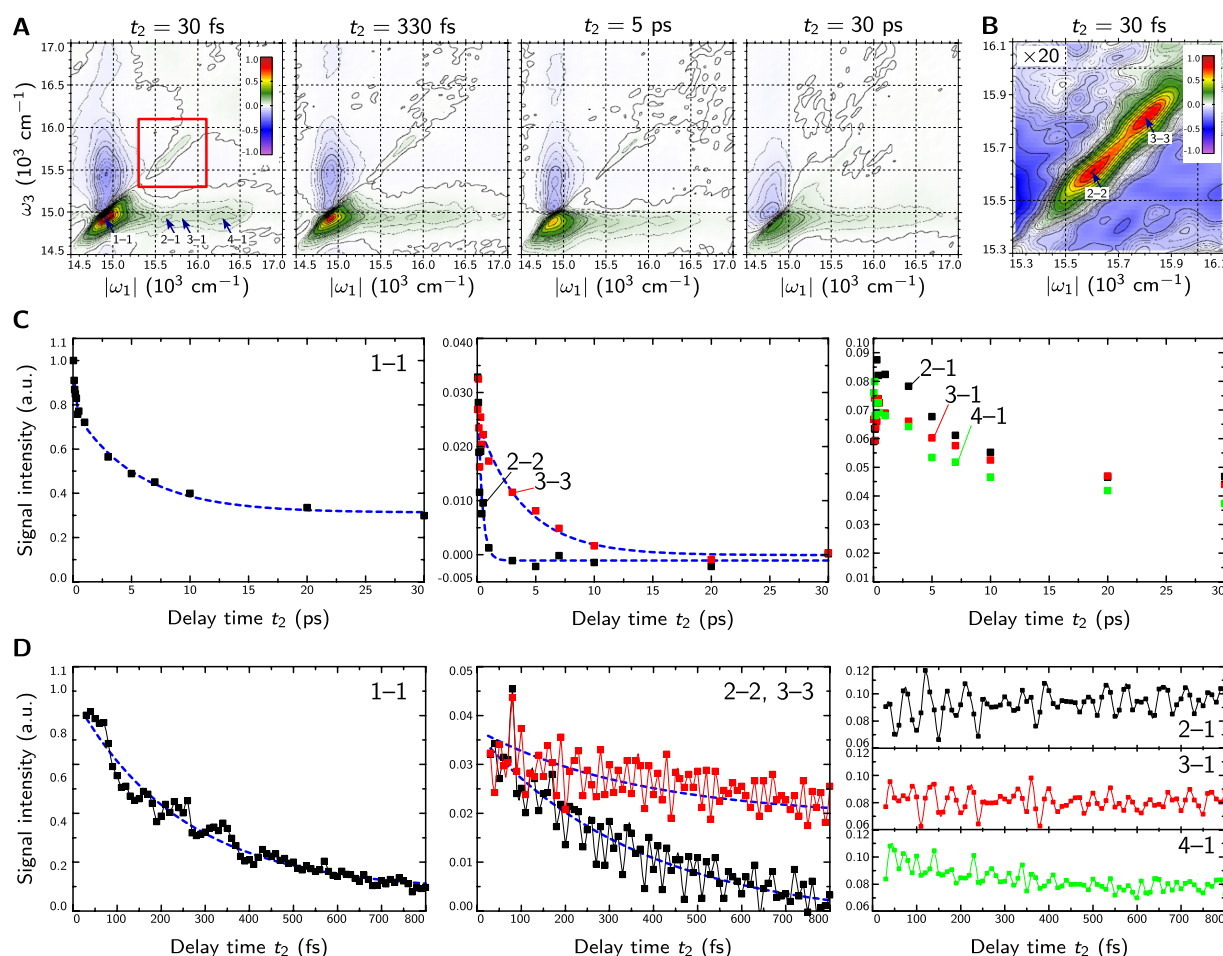

FIG. 2. (a) 2D absorptive spectra at different delay times. All the spectra are normalized to the maximum of the spectrum at $t_2 = 30$ fs and drawn using the same color scale. Thicker contour lines are drawn at every 10% of the maximum of the scale; thinner lines are drawn every 2%, up to $\pm 20\%$. (b) The zoomed-in two-peak structure in the 2D spectrum of FCP, marked in Fig. 2(a) by the red square. Values in the spectrum are multiplied by 20 and the spectrum is drawn using the same color scale as in (a). (c) Picosecond and (d) femtosecond time traces of a few selected peaks indicated by arrows in (a) and (b). Values obtained by averaging around the selected points within the circle of $100\,\mathrm{cm^{-1}}$ radius are presented. Multi-exponential fits of dynamics of a few peaks are shown by the blue dashed lines (see the text for the fitting parameters).
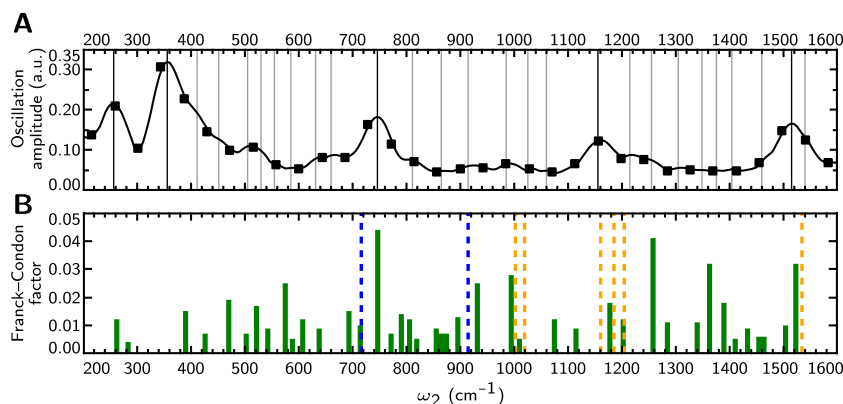
FIG. 3. (a) Amplitude of oscillations (Fourier map norm) as a function of coherence frequency ω_2. Dependency extracted from Fourier transforms of zero-padded and not-padded spectral time evolutions is shown by symbols and lines, respectively. Determined frequencies of oscillations are shown by the vertical black and gray lines. (b) Franck–Condon factors of vibrational intramolecular modes of Chl *a* from the hole burning experiment[31] (green sticks), proposed frequencies of electronic coherences (blue dashed lines), and vibrational Raman frequencies of fucoxanthin[7] (orange dashed lines).

In the region of the Q_y of the Chl *c* transition frequency, i.e., at around $\omega_3 = \omega_1 \approx 15\,700$ cm^{-1}, two diagonal peaks are clearly resolved at excitation/emission frequencies $15\,610$ cm^{-1} and $15\,810$ cm^{-1}. The positions of these peaks are indicated by two vertical bars in the absorption spectrum shown in Fig. 1, coinciding with the maxima of the diagonal cut of the averaged 2D spectrum (black dashed line in Fig. 1). The zoomed-in region of the 2D spectrum from $\omega_3 = \omega_1 = 15\,300$ cm^{-1} to $\omega_3 = \omega_1 = 16\,100$ cm^{-1} (shown by a red square in Fig. 2(a)) is depicted in Fig. 2(b) at delay time $t_2 = 30$ fs. No cross-peak associated with these two transitions is visible at any delay time disproving the presence of excitonic coupling between states at $15\,610$ cm^{-1} and $15\,810$ cm^{-1}.

The 2D spectra contain rich dynamics both at short (femtosecond) and long (picosecond) delay times, as it was extracted from the separate measurements described above. Dynamics of a few selected peaks in the spectra, occurring during first 30 ps, are shown in Fig. 2(c). The main diagonal peak (indicated by "1–1") decays with timescales of 220 ± 100 fs and 5.4 ± 0.6 ps. The cross-peaks (indicated by "2–1," "3–1," and "4–1") decay with the same longer rate of 5.4 ps as the "1–1" peak; the initial evolution is dominated by the high amplitude coherences (Fig. 2(d)) and, thus, shorter lifetimes could not be unambiguously evaluated. Diagonal peaks at $15\,610$ cm^{-1} and $15\,810$ cm^{-1} show completely different long-time dynamics. The upper peak decays much slower than the lower one, as it can be seen by the spectral traces, indicated by "2–2" and "3–3" in Fig. 2(c). We could fit the dynamics of both peaks as single-exponential decays with timescales of 320 ± 70 fs and 3.9 ± 1.6 ps, respectively. For longer delay times, additional exponential decays are present.

The short-time (femtosecond) evolution of the same points in the spectrum is shown in Fig. 2(d) demonstrating the oscillating behavior of the diagonal and off-diagonal peaks corresponding to the Chl *a*. Coherence beatings can be analyzed by performing the Fourier transform of the time traces of the peaks. A very convenient way to represent the overall complexity of oscillations in the 2D spectrum is through the Fourier maps.[36–41] They are constructed by performing the Fourier transform of the each data point in the 2D spectrum over the delay time t_2 after subtraction of slow exponential decay contributions. Then, the Fourier amplitude can be plotted as a two-dimensional map against the excitation and detection frequencies ω_1 and ω_3 for a fixed Fourier frequency ω_2. Each Fourier map then can be integrated

over ω_1 and ω_3 and the integral value can be represented as a function of coherence frequency ω_2. We chose to represent the amplitude of observed oscillations by the value of the Fourier map norm, which is equal to the square root of the sum of squares of the data points of Fourier maps at frequency ω_2. Such a dependency would show the integrated intensities of various oscillation frequencies. From the oscillation amplitude dependency shown in Fig. 3(a), five sharp peaks at ω_2 = 255 cm^{-1}, 345 cm^{-1}, 745 cm^{-1}, 1155 cm^{-1}, and 1515 cm^{-1} can be readily pointed out. More rigorous analysis of the second derivative of the oscillation amplitude function reveals 24 more frequencies.

IV. DISCUSSION

The 2D ES spectra obtained with femtosecond and picosecond time resolutions give a wealth of information regarding both evolution of populations and coherences of the molecular system. Special attention should be taken into consideration when analyzing the processes occurring on different timescales. Thus, before turning to the analysis of the femtosecond evolution of the measured spectra, let us discuss a few mechanisms that contribute to the spectral lineshape formation: pulse overlap, spectral diffusion, dynamic Stokes shift, and coherence beatings. They can be important factors that might lead to ambiguities and errors when interpreting the time-dependencies of the 2D spectrum.

Pulse overlap effects dominate during the initial delay time evolution, comparable to the length of the laser pulses. That is, besides the double-coherence pathways, additional rephasing contributions appear in the phase matching direction when the $\vec{k}_1$ and $\vec{k}_2$ pulses do overlap.[42] Therefore, the initial evolution of the 2D spectrum (in our case first 30 fs) is dominated by the sharp decay of these additional pulse-overlap contributions and should be considered very carefully as they could be confused with some ultrafast relaxation mechanisms.

Spectral diffusion can also make an evident influence on the 2D spectrum.[43] It accounts for the loss of correlation of the absorption and emission frequencies. Spectral diffusion is manifested by the increase of the anti-diagonal width of the peaks in the absorptive 2D spectrum with the delay time and affects both the rephasing and nonrephasing spectral contributions. For a simple two-level system, the rate of the spectral diffusion can be related to the bath relaxation

time and results in exponential decrease of the height of the main absorption peak in the 2D spectrum.[44] As such an exponential evolution overlaps with the other temporal lineshape formation mechanisms, it becomes troublesome not to overinterpret the spectral diffusion as a population relaxation-type signal. Comparing the evolution of the peak height against its anti-diagonal width provides a possible way to evaluate the contribution of the spectral diffusion. However, sometimes this is not possible because of overlaps of closely positioned states and cross-peaks. The other method is to check the time evolution of the integral over some area of the spectrum in the vicinity of the peak under consideration in the absorptive spectrum. If the radius of the integrated area is larger than the homogeneous linewidth, the spectral diffusion is averaged out from such signal.

System states during the delay time t_2 experience relaxation processes through the vibronic pathways. Such a vibrational cooling is often referred to as the dynamic Stokes shift and expresses itself as the shifting of peaks down in the energy scale along the emission axis with t_2 in the 2D spectrum. As the ground state bleaching (GSB) and stimulated emission (SE) features can, in principle, experience the dynamic Stokes shift on different timescales, it can cause some overlaps of these positive and negative contributions, giving a complex time-dependence of both diagonal peaks and cross-peaks. Moreover, the timescale of the dynamic Stokes shift can be around a few hundreds of femtoseconds—therefore, without a careful analysis, such evolution might once again be wrongly assigned to some ultrafast relaxation pathway.

Finally, the initial evolution of the 2D spectrum is seriously affected by the coherence beatings. Lifetimes of the electronic coherences can be as short as tens of femtoseconds, and vibrational/vibronic coherences can result in oscillations for as long as a few picoseconds. Although the static disorder tends to dephase electronic coherences very quickly, their contribution to the initial dynamics can still be substantial. The coherent signal adding on top of the population evolution can be as significant as the population signal itself. Thus, coherence beatings can seriously impede interpretations of the population dynamics if the 2D spectrum is of low resolution in delay time t_2.

A. Identification of coherences

In the 2D ES spectra of FCP, we would expect coherences of various origins and amplitudes to appear: ground state vibrational coherences of Chl *a*, Chl *c*, and Fx, excited state vibronic coherences of the same frequencies, mixed coherences of shifted or combination frequencies,[16,45] and electronic coherences due to excitonic coupling of chlorophylls. Such distinction between the coherences of different origin is conveniently observed in the Fourier amplitude maps. In the rephasing spectrum, ground state coherences are manifested by strong beatings below and on the diagonal[38] while the corresponding vibronic coherences—above the diagonal.[46–48] Mixed coherences, that represent superpositions of quantum mechanically mixed states, are observed as complex and asymmetric patterns of oscillating peaks in the Fourier maps.[45,48] Electronic coherences in the rephasing spectrum manifest themselves

exclusively as oscillatory cross-peaks and no oscillations on the diagonal and vice versa for the nonrephasing spectrum.[38] However, oscillations in the nonrephasing contribution of the spectrum are more sensitive to the static disorder of pigment energies and, thus, in the systems with large inhomogeneous broadening coherences from the rephasing contributions will dominate over those from the nonrephasing contribution.

Let us discuss about the origin of coherences in the spectra of FCP by comparing the obtained dependencies of the intensity of oscillations (Fig. 3(a)) with known frequencies corresponding to the intramolecular vibrational modes of Chl *a*. We refer to the hole burning experiments on single chlorophylls carried out at 1.6 K by Gillie and Small[31] (green sticks in Fig. 3(b)) and a recent study of Du *et al.*,[35] in which the frequencies were obtained from the time and frequency resolved pump–probe spectra at 297 K by the Fourier analysis, similar to the one employed here.

Frequencies, reported in these studies as well as obtained by our experiment, are summarized in Table I. The comparison gives almost perfect agreement not only for the obtained strongest coherences at around $\omega_2 = 255$ cm^{-1}, 345 cm^{-1}, and 745 cm^{-1} (deviations smaller than 11 cm^{-1}) but also for the weaker ones with the largest deviation of 20 cm^{-1} for

TABLE I. Summary of coherent oscillations (cm^{-1}) in the measured FCP 2D spectrum (first column). Vibrational frequencies of chlorophyll *a* obtained from the hole burning[31] (HB, second column) and pump–probe[35] (PP, third row) experiments. Vibrational frequencies of fucoxanthin from the resonant Raman (RR) study[7] are shown in the fourth row. Numbers in bold denote the five most intensive oscillations in 2D and pump–probe experiments, two most intensive Raman modes of fucoxanthin, and frequencies from the hole-burning experiment, having Franck–Condon factors higher than 0.02.

| FCP	Chl *a* HB	Chl *a* PP	Fx RR	FCP	Chl *a* HB	Chl *a* PP	Fx RR
135	...	...	...	...	864	...	...
190	...	214	...	...	874	...	...
255	262	**259**	...	...	896	...	...
...	283	300	...	915	**932**	915	...
345	...	**346**	...	985	**994**	**982**	1002
...	390	...	...	1025	1009	1043	1019
410	425	407	...	1060	1075	1084	...
450	469	...	...	1114	1124	...	...
505	501	...	...	**1155**	...	...	**1160**
530	521	519	...	...	1178	1175	1185
555	541	**565**	...	1215	1203	...	1205
...	**574**	...	...	1255	**1259**	1252	...
585	588	...	...	1305	1285	...	...
...	607	...	...	1350	1340	1353	...
630	638	621	...	1375	**1364**	...	...
660	...	667	...	...	1390	...	...
...	692	...	...	1405	1411	1415	...
...	714	...	...	...	1433	...	...
745	**746**	**744**	...	...	1455	...	...
...	771	...	...	1460	1465	1460	...
...	791	...	...	...	1504	...	...
810	805	799	...	**1515**	**1524**	1516	...
...	819	...	...	1540	...	...	**1536**
865	855	...	...				
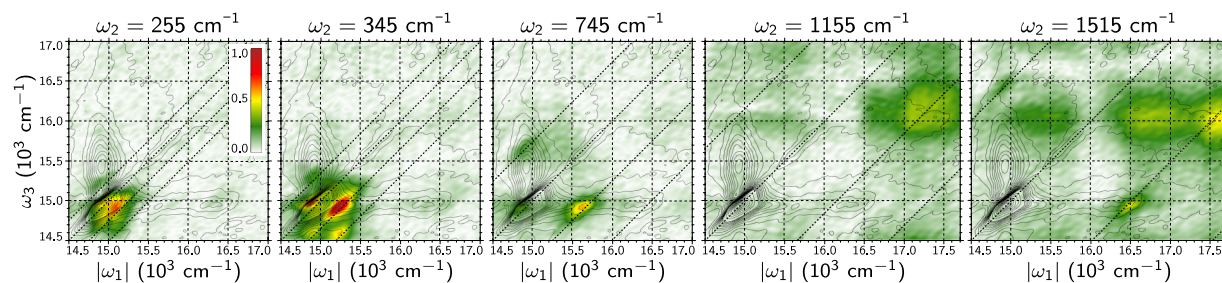
FIG. 4. Fourier amplitude maps at coherence frequencies $\omega_2 = 255$ cm^{-1}, 345 cm^{-1}, 745 cm^{-1}, 1155 cm^{-1}, and 1515 cm^{-1}. Fourier amplitude is shown by a color scale, normalized to the maximum of the map at $\omega_2 = 345$ cm^{-1}. Black contour lines show the 2D spectrum at $t_2 = 30$ fs. Diagonal and parallel to the diagonal dashed lines are shifted by the corresponding value of ω_2. Notice that excitation axes (ω_1) of maps at $\omega_2 = 1155$ cm^{-1} and 1515 cm^{-1} are extended compared to the other maps.

the $\omega_2 = 1305$ cm^{-1} vibrational mode. The Fourier amplitude maps at $\omega_2 = 255$ cm^{-1}, 345 cm^{-1}, and 745 cm^{-1} are shown in Fig. 4. All three of them clearly indicate the presence of vibrational and vibronic coherences as the patterns of the oscillatory features can be easily decomposed to 4 stimulated emission and 4 GSB contributions of a simple two-level system with one vibrational state in the excited and ground states (see the scheme and the corresponding excitation pathways in Figs. 5(a) and 5(c)). From the scheme, it follows that weak features above the diagonal, separated by exactly ω_2 value, indicate vibronic excited state coherences (the SE$_1$ pathway).

The map at $\omega_2 = 745$ cm^{-1} lacks amplitude of oscillations on the diagonal compared to the $\omega_2 = 345$ cm^{-1} or ω_2

= 255 cm^{-1} maps due to the narrow bandwidth of the laser spectrum, suppressing some specific coherences. That is, since Chl a 0–0 transition is on the low-energy shoulder of the laser excitation spectrum, all excitation pathways containing lower energy transitions (indicated by the dashed arrows in Fig. 5(c)) will be substantially suppressed. These particular pathways in Fig. 5(c) are shown in a shaded background.

For oscillations of higher frequencies, the mentioned contributions will be completely excluded. Therefore, the dependency of amplitude of oscillations in Fig. 3(a) should be considered carefully, as the peak heights there do not perfectly represent the amplitudes of all summed pathways, but are rather suppressed for middle and high frequencies.

The Fourier amplitude maps at $\omega_2 = 1155$ cm^{-1} and 1515 cm^{-1} are shown in Fig. 4. They both contain broad features in the region of excitation frequency $\omega_1 = 16\,500 - 17\,000$ cm^{-1} and emission frequency $\omega_3 \approx \omega_1 - 1155$ cm^{-1} and $\omega_3 \approx \omega_1 - 1515$ cm^{-1}, respectively. With our laser spectrum, we could in principle excite the S$_2$ states of some of the "red" fucoxanthins and, possibly, get signatures of carotenoid ground state coherences (from the GSB$_3^{Fx}$ pathway shown in Fig. 5(d)). These contributions would appear as oscillations at the emission frequency, shifted down from the diagonal by the frequency of the vibrational mode. Therefore, we assign these features observed at $\omega_2 = 1155$ cm^{-1} and $\omega_2 = 1515$ cm^{-1} to the ground state vibrational modes of Fx at 1160 cm^{-1} and 1536 cm^{-1}, respectively.[7]

Apart from the Fx vibrational coherence, the Fourier amplitude map at $\omega_2 = 1515$ cm^{-1} shows oscillations at $\omega_3 = 14\,935$ cm^{-1} and $\omega_1 = 16\,550$ cm^{-1} and a corresponding diagonal-symmetric feature. They can be assigned to the Chl a vibrational and vibronic coherences, respectively. Thus, the full pattern of features in the map at $\omega_2 = 1515$ cm^{-1} can be explained by the scheme shown in Fig. 5(b): the two diagonal-symmetric narrow features come from the excited state vibronic and ground state vibrational coherences of Chl a, and the broad feature below the diagonal is due to vibrational ground state coherences of Fx. The other weak features at the emission frequency $\omega_3 \approx 16\,000$ cm^{-1} and excitation frequencies $16\,300 < \omega_1 < 17\,200$ cm^{-1} come from the nonrephasing contribution (not shown). We could not assign them to any sort of excitation pathways involving the known Chl or Fx states.

The Fourier map at $\omega_2 = 1155$ cm^{-1} clearly lacks similar features stemming from Chl a vibrational coherences and
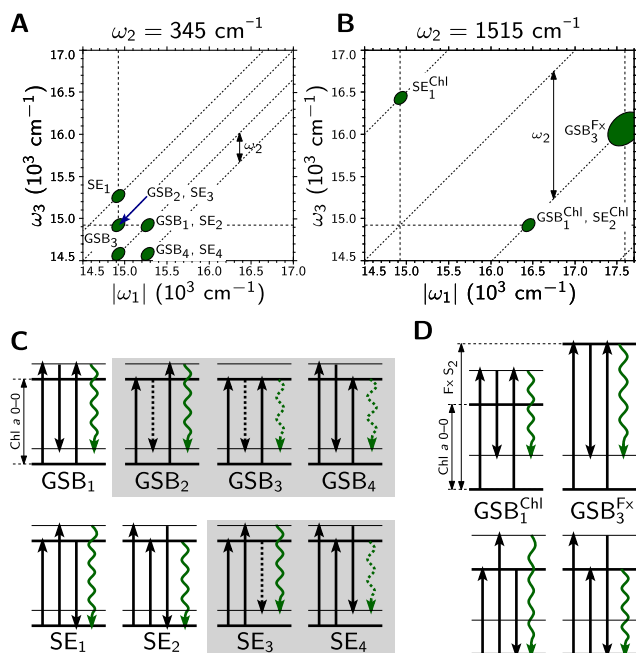

FIG. 5. Patterns of features in the Fourier amplitude maps at $\omega_2 = 345$ cm^{-1} (a) and $\omega_2 = 1515$ cm^{-1} (b). Excitation pathways, leading to coherences in these maps are shown in (c) and (d), respectively. Horizontal thick lines in (c) and (d) show ground and excited state energies of Chl a and Fx. Thin horizontal lines indicate the corresponding vibrational states. Vertical straight arrows represent transitions; vertical wavy lines indicate emission. Transitions, suppressed by the laser spectrum are shown by straight and wavy dashed lines; the pathways, which become negligible for the higher frequency vibrational modes, are shown in the shaded background.

there is no vibrational mode of similar frequency suggested by the hole burning or pump–probe experiments considered here.[31,35] However, the vibrational Chl *a* mode of 1145 cm^{-1} has been reported in the fluorescence line narrowing and resonant Raman study by Telfer *et al.*[49] It is possible that we were not able to resolve signatures of this particular vibrational coherence because of the suppression of high frequency coherences by the laser spectrum as discussed above. Alternatively, there could be additional mechanisms, responsible for some vibrational Chl *a* frequencies not being detected in FCP, e.g., vibronic coupling between Chl *a* in FCP, adding more complexity to spectra, similar to the enhancement of the ground state coherence proposed by Chenu *et al.*,[50] or the anharmonicity of the electron-vibrational coupling recently proposed for the LH2 antennae.[51] Obviously, the situation calls for more detailed study of the vibrational/vibronic coherences of chlorophylls in pigment–protein complexes.

After performing analysis of the Fourier maps of the other coherences, we were not able to extract any oscillatory features that could be assigned to the vibrational/vibronic coherences of Chl *c*. This is probably due to weak signal. Indeed, the Chl *c* absorption signal is at least 5 times weaker than the main absorption band of Chl *a*. Thus, the signal of coherent oscillations might become too weak to be distinguished from the experimental noise. A close inspection of oscillations around the proposed Q$_y$ transition band of Chl *c* (~15 600 cm^{-1}) revealed only very weak signatures of vibrational coherences of Chl *a* and Fx. The former might be coming from the nonrephasing vibrational contribution and the latter—from the overlap of a wide peak of the fucoxanthin ground state vibrational coherence.

Obviously, the strongest high-frequency electronic coherence in the spectra of FCP would be the coherence of Q$_y$ transitions of excitonically coupled Chl *c* and Chl *a*. From the position of the corresponding peaks in the absorption spectrum, the frequency of such a coherence should be around 715 cm^{-1} or 915 cm^{-1}. By comparing the peak heights and assuming that the Franck–Condon factors of vibrational transitions are as small as 0.05, it could easily be deduced that the amplitude of electronic coherence should be higher than the vibrational coherence of Chl *c*. But the dephasing rate of the electronic coherences is known to be much shorter than the vibrational ones.[48] This would prevent the electronic coherence to be captured by the Fourier maps, except of a few cases. One of them is the inhomogeneous distribution induced picosecond electronic coherence lifetime, as it was recently shown by Dong and Fleming.[52] In the inhomogeneously broadened spectrum, the sub-ensemble of molecules having similar energies provides the long-lived coherent signal in the two-color photon echo experiment. Such mechanism could also be significant in the 2D electronic spectroscopy; however, it requires the absorption spectra of Chl *c* and Chl *a* to overlap significantly.

Another mechanism allowing for long-lived electronic coherences is substantial electronic-vibrational mixing in the excited state, resulting in a vibrational coherence lifetime borrowing mechanism.[47] For this effect to be noticeable, the excitonic energy gap between the excitonic states should closely match some strong discrete vibrational mode. In our case, the proposed excitonic energy gap is close to a very strong vibrational modes of 745 cm^{-1} or 915 cm^{-1}, and in the Fourier amplitude maps, the ground state vibrational contribution dominates. Therefore, if there are any observable signatures of electronic coherence beatings, they are hindered by strong features of vibrational coherences.

B. Ultrafast Chl *c*–Chl *a* transfer

In our previous study of the 2D spectra of the FCP complex at room temperature, the ultrafast energy transfer (occurring on timescale of 60 fs) from excitonically coupled Chl *c* to Chl *a* was proposed.[12] It was obtained by tracing the time dynamics of the spectral feature at $\omega_3 = \omega_1$ = 15 680 cm^{-1}, assigned to the Q$_y$ transition of Chl *c*. Here, we report that there are two peaks at 15 610 cm^{-1} and 15 810 cm^{-1} instead of one. This doublet was not resolved in the experiment at room temperature. Moreover, we found significant differences in their decay dynamics. Considering the delay times up to 30 ps, the lower peak decays with the timescale of 320 fs, while the shortest temporal dynamics of the upper peak is 3.9 ps. The timescales were obtained from the delay time traces, taken by averaging over the area of a circle of 100 cm^{-1} radius in spectra and omitting the first 30 fs, thus limiting amount spectral diffusion and pulse overlap contributions appearing in peak dynamics. We conclude that the obtained two different Chl *c* states directly transfer energy to Chl *a* on different timescales. Notice that energy transfer via intermediate states (presumably from fucoxanthins) is not consistent with fluorescence-excitation spectrum of FCP,[5] which implies 100% efficiency of Chl *c* to Chl *a* energy transfer, and the fact that significant portions of excitation from Fx S$_1$/ICT (internal charge transfer) state, which could be suggested to be a bridge between Chl *c* and Chl *a*, are lost due to the decay to the ground state.[25]

Recent studies suggest that there are two Chl *c* molecules in the complex.[7] Also, some of them can be of different types (i.e., Chl c_1, c_2, or c_3) that have slightly different absorption spectra.[53] Even if the discussed spectral features are caused by the chlorophylls of different types (thus, causing signals in different frequencies), temporal dynamics of the corresponding peaks indicate that their interaction with the rest of the system or a surrounding environment is different. The simplest picture is that one Chl *c* is situated in the periphery of the FCP complex and is weakly coupled to the rest of Chl *a*; thus, the excitation transfer to the core pigments is slow and we observe a picosecond decay of the peak at 15 810 cm^{-1}. At the same time, the protein environment causes it to have higher energy. Another, internal Chl *c*, absorbing at 15 610 cm^{-1}, must be coupled to Chl *a* stronger for faster excitation transfer. Since the cross-peak between these two transitions as well as the relevant excited state absorption contribution is absent, the two Chls *c* in FCP are not coupled. This implies that they probably are spatially well separated.

However, the ultrafast energy transfer from the internal Chl *c* state still remains an issue to be explained. The strength of coupling between the Chl *c* and Chl *a* is not known, although it may be estimated from LHCII, which shares considerable sequence homology.[4] Couplings between chlorophylls in the
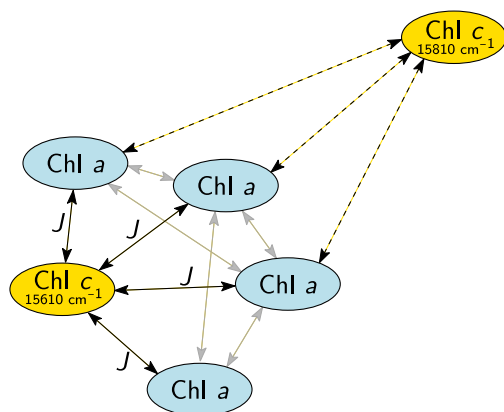
FIG. 6. Proposed functional scheme of spatial arrangement of Chl *c* and *a* molecules in the FCP complex. Couplings between pigments are shown by solid lines. Dashed lines indicate weaker coupling between spatially separated Chl *c* absorbing at $15\,810$ cm^{-1}. Chl *a* molecules shown here do not represent their actual number in FCP.

LHCII complex were calculated to be less than 100 cm^{-1}.[54] Considering this and the fact that the transition dipole moment of the Q_y band is smaller for Chl *c* than for Chl *a*, one can be certain that coupling between Chl *c* and Chl *a* in FCP should be even weaker. This is also supported by the absence of clear excitonic cross-peaks between Chl *a* and Chl *c* states in our 2D spectra.

The Förster energy transfer could apply in this range of parameters. However, it leads to slower—picosecond—transfer rates. The 320 fs transfer timescale observed in 2D ES could be explained by using a structural model shown in Fig. 6 and including two ingredients into the consideration. First, the internal Chl *c* can be coupled to several Chl *a* molecules; thus, it transfers energy to a few Chl *a* molecules at once. The rates effectively sum-up and lead to the fast decay of the Chl *c* population. Second, vibrations-assisted energy transfer enhancement might be significant for the Chl *c*–Chl *a* energy transfer.[55] The energy gap of 715 cm^{-1} is close to the strongest vibrational Chl *a* mode of 745 cm^{-1}, thus allowing for electronic-vibrational resonance.[56–58] Finally, this does not contradict our previous suggestion that this Chl *c* is coherently coupled to Chl *a*;[12] however, the coherent mechanism may be far more complicated and calls for future studies.

The proposed schematic spatial arrangement of Chl *a* and Chl *c* molecules (shown in Fig. 6) is comparable to the CP29 photosynthetic antenna of photosystem II (PSII).[59,60] The structure of the CP29 complex is similar to the LHCII complex, which shares the sequence homology with FCP. In CP29, there are eight Chl *a* and four Chl *b* (the absorption maximum of Chl *b* is around $15\,674$ cm^{-1}, similarly as to Chl *c*) and one more chlorophyll binding site can be occupied by either type of chlorophyll,[60] although previously it was assumed that there are 8 Chl *a* and 2 Chl *b* molecules.[59] However, in both models, one Chl *b* molecule is well spatially separated from the other which is strongly coupled to the rest of the Chls *a* of the complex. Consequentially, two absorption bands at $15\,650$ cm^{-1} and $15\,385$ cm^{-1} are observed in the absorption and in the pump–probe spectrum have completely different temporal dynamics: the energy transfer from Chl *b* at higher energy is transferred to Chl *a* with the rate of

350 fs, while transfer from the lower energy Chl *b* band occurs in 2.2 ps.[59] This implies that having two accessory chlorophylls that are in different spatial situations might be a property shared by a number of light-harvesting complexes; thus probably it has a functional significance.

In a recent study of FCP based on resonance Raman technique,[7] signatures of two distinct Chl *c* molecules were observed. In that study, a possible pigment organization scheme in FCP was discussed, based on the pigment binding sites of LHCII from plants.[10] It was suggested that one of Chl *c* should be bound at either the site of a614 (which is preserved in FCP) or a613 (not preserved in FCP), while the other Chl *c* should be bound at the site of b609 (preserved) or a604 (not preserved). For the internal Chl *c*, the site of b609 would be a logical choice, as it is in the vicinity of several pigments. Meanwhile, the peripheral ($15\,810$ cm^{-1}) Chl *c* could indeed be situated at the site of a614, as that site is relatively isolated and would be in accord with slower energy transfer from this pigment. Since this pigment is situated at the periphery of the complex, it might be responsible for the inter-complex Chl *c* to Chl *a* transfer in the FCP–PSII supercomplexes.[61]

V. CONCLUSIONS

In this work, we studied low-temperature and high-resolution experimental two-dimensional spectra of the FCP complex. Short time (femtosecond) dynamics of the spectra show complex oscillation patterns. They are dominated by vibrational and vibronic coherences of Chl *a* and fucoxanthin; electronic coherences could not be identified due to their short lifetime and being hindered under high-amplitude oscillations originating from Chl *a*. Most notably, we have resolved two distinct states that can be assigned to Chls *c*. These states were not found in the previous studies of FCP and their energies were not known. The two Chl *c* molecules transfer energy to Chl *a* with rates that differ by about an order of magnitude. We suggest that the lower energy Chl *c* molecule is situated in the core of the complex and is coupled to an aggregated pool of Chl *a* molecules and the Chl *c*-to-*a* energy transfer might be vibronically enhanced. The other Chl *c* should be in the periphery of the complex to transfer energy on the picosecond timescale.

[1]P. G. Falkowski, R. T. Barber, and V. Smetacek, Science **281**, 200 (1998).

[2]C. B. Field, M. J. Behrenfeld, J. T. Randerson, and P. Falkowski, Science **281**, 237 (1998).

[3]D. G. Mann, Phycologia **38**, 437 (1999).

[4]M. Eppard and E. Rhiel, Mol. Gen. Genet. **260**, 335 (1998).

[5]E. Papagiannakis, I. H. M. van Stokkum, H. Fey, C. Büchel, and R. van Grondelle, Photosynth. Res. **86**, 241 (2005).

[6]C. Wilhelm, C. Büchel, J. Fisahn, R. Goss, T. Jakob, J. LaRoche, J. Lavaud, M. Lohr, U. Riebesell, K. Stehfest, K. Valentin, and P. G. Kroth, Protist **157**, 91 (2006).

[7]L. Premvardhan, B. Robert, A. Beer, and C. Büchel, Biochim. Biophys. Acta, Bioenerg. **1797**, 1647 (2010).

[8]N. Gildenhoff, J. Herz, K. Gundermann, C. Büchel, and J. Wachtveitl, Chem. Phys. **373**, 104 (2010).

[9]L. Premvardhan, L. Bordes, A. Beer, C. Büchel, and B. Robert, J. Phys. Chem. B **113**, 12565 (2009).

[10]Z. Liu, H. Yan, K. Wang, T. Kuang, J. Zhang, L. Gui, X. An, and W. Chang, Nature **428**, 287 (2004).

[11]R. Croce and H. van Amerongen, Nat. Chem. Biol. **10**, 492 (2014).

[12]E. Songaila, R. Augulis, A. Gelzinis, V. Butkus, A. Gall, C. Büchel, B. Robert, D. Zigmantas, D. Abramavicius, and L. Valkunas, J. Phys. Chem. Lett. **4**, 3590 (2013).

[13]T. Brixner, J. Stenger, H. M. Vaswani, M. Cho, R. E. Blankenship, and G. R. Fleming, Nature **434**, 625 (2005).

[14]G. S. Schlau-Cohen, T. R. Calhoun, N. S. Ginsberg, E. L. Read, M. Ballottari, R. Bassi, R. van Grondelle, and G. R. Fleming, J. Phys. Chem. B **113**, 15352 (2009).

[15]A. Gelzinis, L. Valkunas, F. D. Fuller, J. P. Ogilvie, S. Mukamel, and D. Abramavicius, New J. Phys. **15**, 075013 (2013).

[16]F. D. Fuller, J. Pan, A. Gelzinis, V. Butkus, S. S. Senlik, D. E. Wilcox, C. F. Yocum, L. Valkunas, D. Abramavicius, and J. P. Ogilvie, Nat. Chem. **6**, 706 (2014).

[17]E. Romero, R. Augulis, V. I. Novoderezhkin, M. Ferretti, J. Thieme, D. Zigmantas, and R. van Grondelle, Nat. Phys. **10**, 676 (2014).

[18]H. Lee, Y.-C. Cheng, and G. Fleming, Science **316**, 1462 (2007).

[19]D. Zigmantas, E. L. Read, T. Mančal, T. Brixner, A. T. Gardiner, R. J. Cogdell, and G. R. Fleming, Proc. Natl. Acad. Sci. U. S. A. **103**, 12672 (2006).

[20]J. Dostál, T. Mančal, R. Augulis, F. Vácha, J. Pšenčík, and D. Zigmantas, J. Am. Chem. Soc. **134**, 11611 (2012).

[21]J. M. Anna, E. E. Ostroumov, K. Maghlaoui, J. Barber, and G. D. Scholes, J. Phys. Chem. Lett. **3**, 3677 (2012).

[22]E. Collini and G. D. Scholes, Science **323**, 369 (2009).

[23]F. Milota, J. Sperling, A. Nemeth, and H. F. Kauffmann, Chem. Phys. **357**, 45 (2009).

[24]D. B. Turner, Y. Hassan, and G. D. Scholes, Nano Lett. **12**, 880 (2012).

[25]A. Gelzinis, V. Butkus, E. Songaila, R. Augulis, A. Gall, C. Büchel, B. Robert, D. Abramavicius, D. Zigmantas, and L. Valkunas, Biochim. Biophys. Acta, Bioenerg. **1847**, 241 (2015).

[26]C. Büchel, Biochemistry **42**, 13027 (2003).

[27]T. Brixner, I. V. Stiopkin, and G. R. Fleming, Opt. Lett. **29**, 884 (2004).

[28]R. Augulis and D. Zigmantas, Opt. Express **19**, 13126 (2011).

[29]J. D. Hybl, A. W. Albrecht, S. M. G. Faeder, and D. M. Jonas, Chem. Phys. Lett. **297**, 307 (1998).

[30]D. M. Jonas, Annu. Rev. Phys. Chem. **54**, 425 (2003).

[31]J. K. Gillie and G. J. Small, J. Phys. Chem. **93**, 1620 (1989).

[32]V. Butkus, A. Gelzinis, and L. Valkunas, J. Phys. Chem. A **115**, 3876 (2011).

[33]D. Abramavicius, Europhys. Lett. **101**, 57007 (2013).

[34]J. Han, H. Zhang, and D. Abramavicius, J. Chem. Phys. **139**, 034313 (2013).

[35]J. Du, T. Teramoto, K. Nakata, E. Tokunaga, and T. Kobayashi, Biophys. J. **101**, 995 (2011).

[36]G. Panitchayangkoon, D. Voronine, D. Abramavicius, J. Caram, N. Lewis, S. Mukamel, and G. Engel, Proc. Natl. Acad. Sci. U. S. A. **108**, 20908 (2011).

[37]H. Li, A. D. Bristow, M. E. Siemens, G. Moody, and S. T. Cundiff, Nat. Commun. **4**, 1390 (2013).

[38]V. Butkus, D. Zigmantas, L. Valkunas, and D. Abramavicius, Chem. Phys. Lett. **545**, 40 (2012).

[39]J. Seibt and T. Pullerits, J. Phys. Chem. C **117**, 18728 (2013).

[40]M. Ferretti, V. I. Novoderezhkin, E. Romero, R. Augulis, A. Pandit, D. Zigmantas, and R. Grondelle, Phys. Chem. Chem. Phys. **16**, 9930 (2014).

[41]F. V. A. Camargo, H. L. Anderson, S. R. Meech, and I. A. Heisler, J. Phys. Chem. A **119**, 95 (2014).

[42]D. Abramavicius, V. Butkus, J. Bujokas, and L. Valkunas, Chem. Phys. **372**, 22 (2010).

[43]D. Abramavicius, L. Valkunas, and S. Mukamel, Europhys. Lett. **80**, 17005 (2007).

[44]P. Hamm and M. Zanni, *Concepts and Methods of 2D Infrared Spectroscopy* (Cambridge University Press, 2011).

[45]V. Butkus, J. Alster, E. Bašinskaitė, R. Augulis, P. Neuhaus, L. Valkunas, H. L. Anderson, D. Abramavicius, and D. Zigmantas "Diversity of coherences and origin of electronic transitions of supermolecular nanoring," preprint arXiv:1503.00870 (2015).

[46]V. I. Novoderezhkin, E. G. Andrizhiyevskaya, J. P. Dekker, and R. van Grondelle, Biophys. J. **89**, 1464 (2005).

[47]V. Butkus, D. Zigmantas, D. Abramavicius, and L. Valkunas, "Role of coherent vibrations in energy transfer and conversion in photosynthetic pigment-protein complexes," Photosynth. Res. **587**, 93 (published online) (2013).

[48]V. Butkus, L. Valkunas, and D. Abramavicius, J. Chem. Phys. **140**, 034306 (2014).

[49]A. Telfer, A. A. Pascal, L. Bordes, J. Barber, and B. Robert, J. Phys. Chem. B **114**, 2255 (2010).

[50]A. Chenu, N. Christensson, H. F. Kauffmann, and T. Mančal, Sci. Rep. **3**, 2029 (2013).

[51]O. Rancova and D. Abramavicius, J. Phys. Chem. B **118**, 7533 (2014).

[52]H. Dong and G. R. Fleming, J. Phys. Chem. B **118**, 8956 (2014).

[53]D. Kosumi, M. Kita, R. Fujii, M. Sugisaki, N. Oka, Y. Takaesu, T. Taira, M. Iha, and H. Hashimoto, J. Phys. Chem. Lett. **3**, 2659 (2012).

[54]C. D. P. Duffy, J. Chmeliov, M. Macernis, J. Sulskus, L. Valkunas, and A. V. Ruban, J. Phys. Chem. B **117**, 10974 (2013).

[55]D. Abramavicius and L. Valkunas, "Role of coherent vibrations in energy transfer and conversion in photosynthetic pigment-protein complexes," Photosynth. Res. (published online).

[56]F. Caruso, A. W. Chin, A. Datta, S. F. Huelga, and M. B. Plenio, J. Chem. Phys. **131**, 105106 (2009).

[57]J. Womick and A. Moran, J. Phys. Chem. B **115**, 1347 (2011).

[58]A. Kolli, E. O'Reilly, G. Scholes, and A. Olaya-Castro, J. Chem. Phys. **137**, 174109 (2012).

[59]C. C. Gradinaru, A. A. Pascal, F. van Mourik, B. Robert, P. Horton, R. van Grondelle, and H. van Amerongen, Biochemistry **37**, 1143 (1998).

[60]X. Pan, M. Li, T. Wan, L. Wang, C. Jia, Z. Hou, X. Zhao, J. Zhang, and W. Chang, Nat. Struct. Mol. Biol. **18**, 309 (2011).

[61]S. Akimoto, A. Teshigahara, M. Yokono, M. Mimuro, R. Nagao, and T. Tomo, Biochim. Biophys. Acta, Bioenerg. **1837**, 1514 (2014).